Astronomy Reports, Vol. 46, No. 9, 2002, pp. 712–720. Translated from Astronomicheskiĭ Zhurnal, Vol. 79, No. 9, 2002, pp. 787–797.

$BVRI$Hα CCD Photometry of the Spiral Galaxy NGC 3184

A. S. Gusev[1,2,3,4] and S. S. Kaĭsin[5]

[1] *Sternberg Astronomical Institute, Universitetskiĭ pr. 13, Moscow, 119899 Russia*
[2] *Kyungpook National University, Taegu 702-701, Korea*
[3] *Institute of Solid State Physics, P.O. Chernogolovka, Moscow region, 142432 Russia*
[4] *Astronomy Data Center, University of Cambridge, Cambridge, Great Britain*
[5] *Special Astrophysical Observatory, Russian Academy of Sciences, Nizhniĭ Arkhyz, Karachaevo-Cherkesskaya Republic, 357147 Russia*

Received November 19, 2001; in final form, February 1, 2002

Abstract—We have carried out $BVRI$Hα CCD surface photometry of the spiral galaxy with active star formation NGC 3184 using the 1-m telescope of the Special Astrophysical Observatory. B and Hα data from the ING Archive (La Palma Observatory) were also used. We consider the structure and radial brightness distribution of the galaxy. Stellar populations in different regions of the galaxy are analyzed using two-color diagrams. We have identified and studied star-forming regions in NGC 3184 and estimated their ages based on evolutionary modeling.

1. GENERAL INFORMATION

NGC 3184 is a relatively nearby, late-type barred spiral galaxy viewed face-on (Fig. 1). Table 1 presents the basic parameters of the galaxy taken from the RC3 Catalog [1].

NGC 3184 has been studied relatively thoroughly, but its morphology and the photometric properties of its components in the VRI bands had not been analyzed in detail. NGC 3184 displays a diffuse core [2, 3] with signs of activity, e.g., Hα emission [2]. The brightness of the galactic disk falls off exponentially; the characteristic scale for the disk given by V photometry is $74''$ [45], while R photometry yields $115''$ [5]. The galaxy possesses a massive bulge whose brightness decreases in accordance with a de Vaucouleurs law with effective radius $38''$ [4]. The bulge luminosity is 6% of the integrated luminosity of the galaxy [5]. Two bright symmetrical spiral arms branch in the outer disk of NGC 3184, forming several long extended arms [6]. A short (semi-major axis $0.4'$), broad ($b/a = 0.95$) bar is visible [7–10], whose brightness also falls off exponentially [9, 10]. According to the calculations of [11], the bar is relatively young (10^8 years).

More than 100 HII regions—sites of star formation—have been identified in the galaxy (see the catalog of Hodge [12]). 32 HII regions in NGC 3184 have been studied in detail spectrophotometrically [13–15]. $UBVRI$Hα photometry has been carried out for 13 young clusters in the galaxy [16, 17].

According to [18], the mass of gas in the galaxy is $M(\mathrm{HI}) = 1.8 \times 10^9 M_\odot$ and $M(\mathrm{H_2}) = 8.0 \times 10^8 M_\odot$. The IR luminosity of NGC 3184 is rather high: $L(\mathrm{FIR}) = 2.1 \times 10^9 L_\odot$ and $L(\mathrm{FIR})/L(B) = 0.24$. The mass of dust in the galaxy is $1.2 \times 10^6 M_\odot$ [18].

ROSAT 0.1–2.0 keV observations indicated an excess of radiation by hot gas beyond the optical boundary of the galaxy, as is especially characteristic of gas with temperatures $T \approx 10^6$ K [19]. The supernova rate in NGC 3184 estimated in [19] ($1/30$ yr^{-1}) is consistent with the observations: four supernova

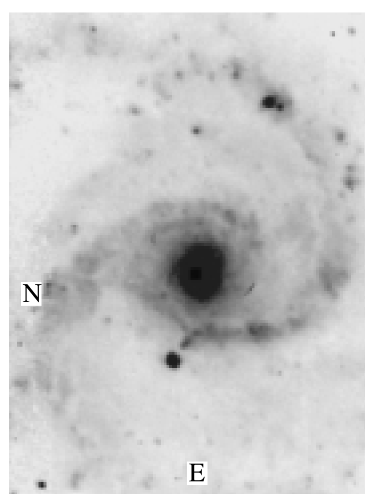

Fig. 1. V CCD image of NGC 3184. The size of the area is $2.4' \times 3.5'$.

outbursts (1921B, 1921C, 1937F, and 1999gi) have been detected over the last century [20, 21].

2. OBSERVATIONS AND REDUCTION

NGC 3184 was observed on January 21–22, 1998, with the 1-m Zeiss-1000 telescope of the Special Astrophysical Observatory (focal length 13.3 m) using a permanently mounted CCD photometer [22]. The photometric system of the K585 CCD camera with V, R, and I broadband filters is close to the standard VRI Johnson–Cousins system. The size of the CCD is 530×580 pixels, which provides a $143'' \times 212''$ field of view for an image scale of $0.28''$/pixel $\times$ $0.37''$/pixel.

Five exposures were made in each filter. Between exposures, the telescope was shifted by several arcseconds to decrease the impact of flaws in the CCD. The duration of one exposure in each filter was 600 s. The seeing was $2.5''$–$3.0''$.

The photometric calibration was carried out using standard stars from the list of [23] (PG0220, PG1407, RU149, S101429), which were observed on the same night. We also used the galactic aperture photometry data of the catalog [24]. The data of [15] were used to calibrate the Hα image.

The preliminary reduction of the images was performed at the Special Astrophysical Observatory. To take into account the electronic bias and the influence of hot pixels, a dark frame was subtracted from the frames obtained for the target and standard stars. This dark frame was averaged from several closed-shutter exposures made with the same integration time as for the target. For the flat field, we used twilight sky integrated in each filter with signal-to-noise ratio no lower than 60–80. All the images were divided by a flat field to take into account the inhomogeneous sensitivity of the detecting elements.

We used B and Hα images of NGC 3184 taken from the archive of the Isaac Newton Group (Astronomy Data Center, University of Cambridge, Great Britain), obtained using the telescopes of La Palma Observatory. The B image was obtained on March 5–6, 1999, at the Cassegrain 1 : 25 focus of the 1-m Jacob Kapteyn Telescope, with the JAC 1124×1124 CCD. The field of the CCD was $338'' \times 338''$, with an image scale of $0''.33$/pixel. The duration of the exposure was 900 s. The Hα image of NGC 3184 ($\lambda_0 =$ 6577 Å) was acquired on January 15–16, 1998 with the 4.2-m William Hershel Telescope (Cassegrain focus), using a TEK-5 CCD array. The size of the CCD was 1124×1124 pixel, with an image scale of $0''.30$/pixel. The duration of the exposure was 900 s.

Further, all images were processed at the Sternberg Astronomical Institute using the standard ESO MIDAS procedures. The basic stages of the image processing were as follows.

Table 1. Basic parameters of NGC 3184

Parameter	Value
Type	SBc
m_B, mag	10.42
$M_B^{0,i}$, mag	−19.81
V_{LG}, km/s	605
R, Mpc ($H_0 = 75$ km s^{-1}Mpc^{-1})	8.07
D_{25}, arcmin	7.85
i, deg	24.2
PA, deg	135

Table 2. Reddening due to Galactic absorption and absorption due to the inclination of NGC 3184

Color index	E	E_i
$B - V$	0.06	0.009
$V - R$	0.03	0.004
$R - I$	0.04	0.006

(a) Reducing the images to a single scale ($0.37''$/pixel) and bringing the images of the galaxy into coincidence with an accuracy of up to 0.1 pixel. Shifting the images between consecutive frames made it possible to effectively eliminate the influence of cosmic ray tracks, individual “hot” pixels, and “bad” columns of the K585 array.

(b) Summing the images of the galaxy made in a single filter.

(c) Correcting for the air mass.

(d) Determining the sky background and subtracting it.

(e) Translating the readings onto a logarithmic scale (magnitudes per square arcsecond) in accordance with the photometric calibration (for the Hα image of the galaxy, relative calibration with a conventional zero point was carried out).

(f) Correcting for differences between the instrumental photometric systems and the standard Johnson–Cousins system (taking into account the color equations obtained).

(g) Subtracting the images obtained in different filters, i.e., color-index mapping of the galaxy.

The sky background for the V, R, and I images of the galaxy was determined from the images of other galaxies obtained on the same night, with corrections for the time of observation and the air mass. The accuracy of the photometric calibration was 0.07^m in B, 0.05^m in V and R, and 0.02^m in I. The relative accuracy for the Hα flux determination was 20%.

All the data (brightness, color indices, Hα luminosity) were corrected for Galactic absorption, and the data for the two-color diagrams and the analysis of the color characteristics of site of star formation in the galaxy were also corrected for absorption due to the inclination of NGC 3184. The correction was introduced according to the standard procedure adopted in the RC3 Catalog [1]. Table 2 presents the absorption in various filters.

Given the accepted distance to the galaxy, the image scale is 14.5 pc/pixel.

3. RESULTS

The size of NGC 3184 exceeds the field of our CCD array. As a result, we are not able to study the ends of the spiral arms and the outer regions of the disk of the galaxy here.

3.1. Photometric Profiles and Morphology of the Galaxy

NGC 3184 possesses a large, bright core (Figs. 2a, 2b). We estimate its diameter to be 0.5 kpc (13″); however, it is not possible to draw a distinct line of demarcation between the core and bulge of the galaxy. The Hα luminosity of the core region within 6.5″ of the center is $3.6 \times 10^5 L_\odot$.

The bulge can be seen out to 0.51 kpc (15″) from the center. The short, faint bar of NGC 3184 is almost perpendicular to its major axis (Fig. 2c). The semimajor axis of the bar is 0.9 kpc (23″), and its position angle is PA $= 90° \pm 2°$ (Fig. 3b). The brightness falls off exponentially along the bar major axis (Fig. 2b); however, it is difficult to distinguish the short bar against the bright bulge. The mean V surface brightness of the bar is 20.8 ± 0.1^m/arcsec^2. At the eastern edge of the bar, the brightness locally increases to $\mu_V = 20.70 \pm 0.05^m$/arcsec^2 (Figs. 2b–2d).

Two bright, weakly-curved spiral arms emerge from the edges of the bar (Figs. 1, 2c, 2d). The arm emerging from the eastern end of the bar (the southern arm) is, on average, 0.2^m/arcsec^2 brighter in V than the northern arm; the surface brightnesses of the arms μ_V are 21.2 ± 0.6 and 21.4 ± 0.6^m/arcsec^2, respectively. Both spiral arms display numerous bright regions with V surface brightnesses up to 19.1^m/arcsec^2 and diameters from 100 to 300 pc (from 3″ to 7″)—sites of active star formation. Some dust lanes are visible along the spiral arms (Fig. 1). Apart from the two main spiral arms, the galaxy also possesses several fainter arms (Figs. 1, 2c, 2d). The V surface brightness of the disk of NGC 3184 does not exceed 22.0^m/arcsec^2.

A very bright star-like object located 1.7 kpc (44″) to the east of the core of NGC 3184 (Figs. 1, 2c, 2d) is of considerable interest. Its maximum V brightness reaches 17.0^m/arcsec^2, and its diameter is 260 pc (6.5″). Figures 1 and 2c, 2d clearly show a bright bridge about 250 pc (6.3″) in length extending from the spiral arm towards the galaxy.

The Hα emission is primarily observed in the core, the circumnuclear region, and the spiral arms of the galaxy (Fig. 2d). The intensity of the emission from these regions exceeds 1.5×10^{-17} erg s^{-1}cm^{-2}, reaching $(3–4) \times 10^{-16}$ erg s^{-1}cm^{-2} in the core and in the bright region in the spiral arm to the southwest of the center of NGC 3184.

We were able to study the dependence of the isophote ellipticity and position angle on distance from the center of the galaxy with good accuracy only within 2.3 kpc (60″) of the center. In the central regions ($r < 30''$), the isophotes are essentially circular ($e = 0.10 \pm 0.05$), and the position angle is PA $= 87° \pm 15°$ (Figs. 3a, 3b). For more distant regions, the $e(r)$ and PA(r) dependences are appreciably affected by the bright spiral arms. It is likely that the difference between the ellipticity of the B isophotes and of isophotes at longer wavelengths (Fig. 3a) is related precisely to this. In long-wavelength bands, the isophote ellipticity increases to 0.51 ± 0.02 by $r = 45''$, then decreases slightly (Fig. 3a). The position angle of the galaxy increases smoothly to $22° \pm 6°$ (Fig. 3b). We obtained the overall value $e = 0.23 \pm 0.07$, which corresponds to an inclination for NGC 3184 of $i = 40° \pm 6°$.

Figure 4 presents azimuthally averaged photometric profiles of NGC 3184 derived using the obtained b/a and PA values. The local brightness increase at $r = 44''$ is related to the bright star-like object described above. The profiles indicate some differences between the characteristics of the inner and outer regions of the disk. The decrease in the disk brightness at $r = 20''–38''$ is consistent with an exponential law with scale 1.14 ± 0.02 kpc ($29.2 \pm 0.4''$) and $\mu_V(0) = 20.12 \pm 0.15^m$/arcsec^2. At $r = 50''–78''$, the characteristic scale of the exponential decrease in the disk brightness is 2.02 ± 0.17 kpc ($51.7'' \pm 4.5''$), and the central surface brightness is $\mu_V(0) = 20.77 \pm 0.13^m$/arcsec^2. When the profiles of the central regions are decomposed into the disk and bulge, it is apparent that the main contribution to the luminosity at $r = 4''–12''$ is made by the bulge. The decrease in the bulge brightness follows a de Vaucouleurs law with effective radius

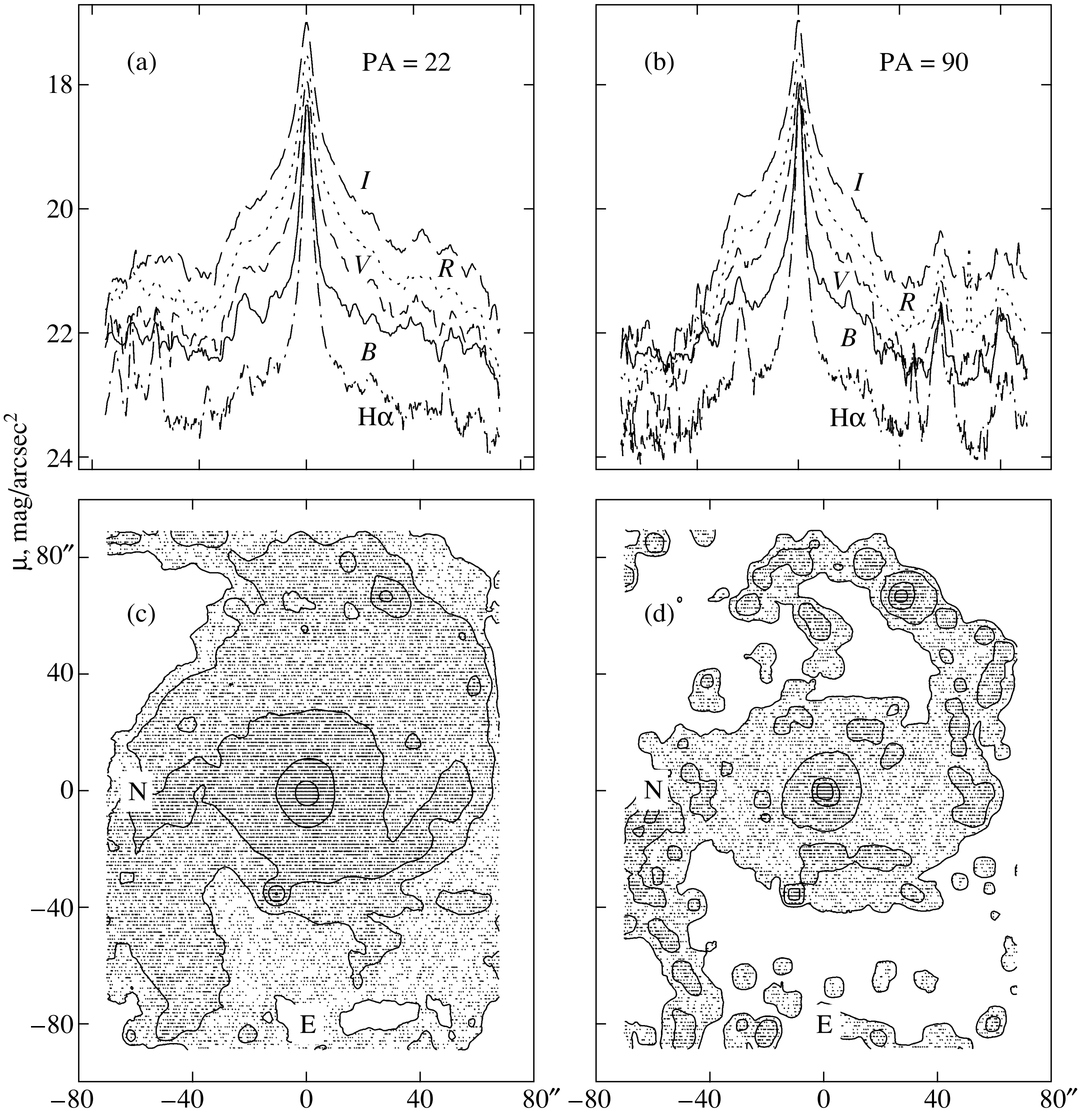

Fig. 2. Photometric profiles (a) along the major axis of the galaxy and (b) along the major axis of its bar in B (solid line), V (short-dashed line), R (dotted line), I (long-dashed line), and Hα (dash-dot line), and images of the galaxy in (c) V and (d) Hα. We have adopted $m_{\mathrm{H}\alpha}(0) = 18^m/\mathrm{arcsec}^2$ for the Hα photometric profiles. The 19.5, 20.5, 21.5, 22.5, and 23.5 isophotes (c) and contours of equal flux at 1.5, 3, 10, and 30 $\times$ 10^{-17} erg s^{-1}cm^{-2} (d) are shown.

0.91 ± 0.14 kpc ($23.2'' \pm 3.7''$) and $\mu_V(r_e) = 25.36 \pm 0.77^m/\mathrm{arcsec}^2$. A King model does not satisfy the observational data for the bulge of NGC 3184. The brightness of the outer disk falls off slightly faster in the I band than in the V and R bands, while the B-band brightness remains virtually constant with distance (Fig. 4). This is due to the presence of a number of bright, blue star-forming regions in the outer disk. As will be shown in Section 3.2, generally speaking, NGC 3184 displays an anomalously large gradient of $B-V$ along the galactic radius.

3.2. Color Distribution

The galaxy as a whole is blue: according to [1, 25], the integrated color indices are $B-V = 0.52 \pm 0.10^m$, $V-R = 0.40 \pm 0.02^m$, and $R-I = 0.50 \pm 0.03^m$. The core of NGC 3184 is moderately red ($B-V = 0.85 \pm 0.10^m$, $V-R = 0.51 \pm 0.07^m$, and $R-I = 0.59 \pm 0.07^m$). The bulge and inner parts of the bar are the reddest regions in NGC 3184 (Figs. 5a–5e). The color indices of the bulge are $B-V = 0.9 \pm 0.1^m$, $V-R = 0.58 \pm 0.03^m$, and $R-I = 0.62 \pm 0.05^m$ (Fig. 5a). The average color indices of the bar are $B-V = 0.65 \pm 0.15^m$, $V-R = 0.54 \pm 0.04^m$, and $R-I = 0.60 \pm 0.03^m$ (Fig. 5b); on average, the bar becomes bluer with distance from

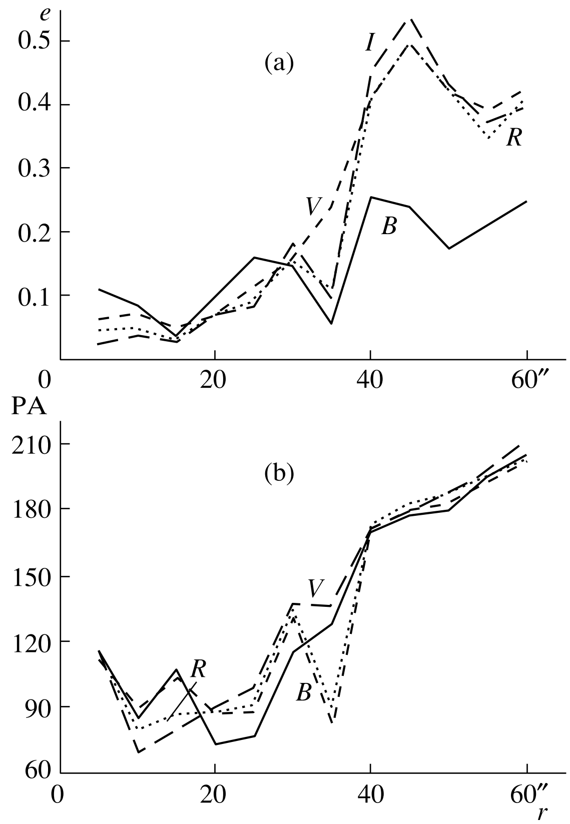

Fig. 3. (a) Isophote ellipticity $e = 1 - b/a$ and (b) position angle of the galaxy PA as a function of the distance r to the center of NGC 3184 in B, V, R, and I.

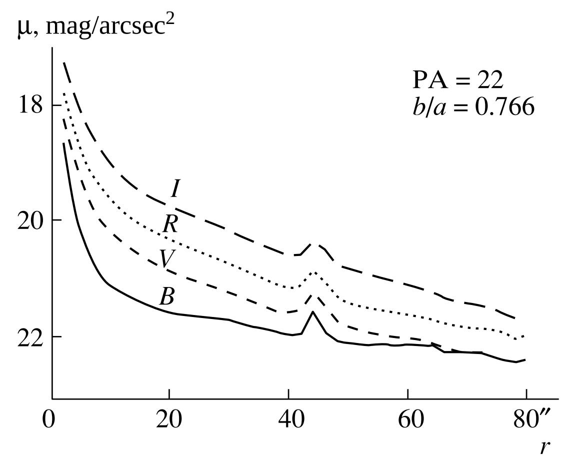

Fig. 4. Mean photometric profiles of NGC 3184 in B, V, R, and I.

the center. The color indices of the disk vary within fairly broad limits. On average, for the disk, $B - V = 0.3 \pm 0.2^m$, $V - R = 0.4 \pm 0.1^m$, and $R - I = 0.55 \pm 0.15^m$ (Figs. 5c–5e). The spiral arms of the galaxy are blue: $B - V = 0.35 \pm 0.10^m$, $V - R = 0.35 \pm 0.05^m$, and $R - I = 0.50 \pm 0.05^m$; the northern and southern spiral arms display the same colors within the errors. The bluest areas in NGC 3184 are bright regions in spiral arms that correspond to sites of star formation. Their photometric characteristics will be considered in detail in Section 3.4.

The large radial gradient of $B - V$ in NGC 3184 is noteworthy (Figs. 5a, 5b). This color index decreases from 0.9 ± 0.1^m in the bulge region (0.3 kpc from the center) to 0.3 ± 0.1^m in the disk region (1.2 kpc from the center).

In general, the distribution of brightness and color in the galaxy is symmetric.

3.3. Two-Color Diagrams

Figure 6a, 6c presents the positions of various regions of NGC 3184 in $(B - V)_0^i - (V - R)_0^i$ and $(B - V)_0^i - (V - I)_0^i$ two-color diagrams. The numbers on the graph denote: 1—the core within 250 pc (6.5″) from the galactic center; 2—the bulge at $r =$ 270–590 pc (7″–15″); 3—the entire galaxy (the integrated color indices are taken from [1, 25]); 4—the spiral arms; 5—the disk; 6–8— bar regions at $r =$ 660, 740, and 820 pc (17″, 19″, and 21″), respectively.

The data in the two-color diagrams have been corrected for absorption due to the inclination of NGC 3184; this is why the color indices for various regions do not coincide with the data presented in Subsection 3.2. Table 2 presents the differences between these values, i.e., the reddening due to the inclination of NGC 3184.

In the $(B - V)_0^i - (V - R)_0^i$ and $(B - V)_0^i - (V - I)_0^i$ diagrams, the dots corresponding to the color indices of various components of the galaxy are located primarily along the normal integrated color sequence (NCS) for galaxies. This testifies to a standard star-formation history in NGC 3184: exponential damping of the star-formation rate at some distance from the center of the galaxy. There is virtually no star formation in the bulge of NGC 3184: its color indices correspond to an aging, metal-deficient stellar system with a characteristic age of several million years. Weak star formation continues in the core of NGC 3184. Active star formation is observed in the spiral arms, the disk, and the outer regions of the bar. The deviation of the color indices of the spiral arms and disk of NGC 3184 to the right of the NCS (points 4 and 5 in Fig. 6a, c) may be due to recent bursts of star formation in these regions—an excess young stellar population compared to the standard population of spiral galaxies is observed. The bar becomes noticeably bluer with distance from the center along the NCS (points 6–8), indicating an increase in the fractional young stellar population toward the periphery of the bar.

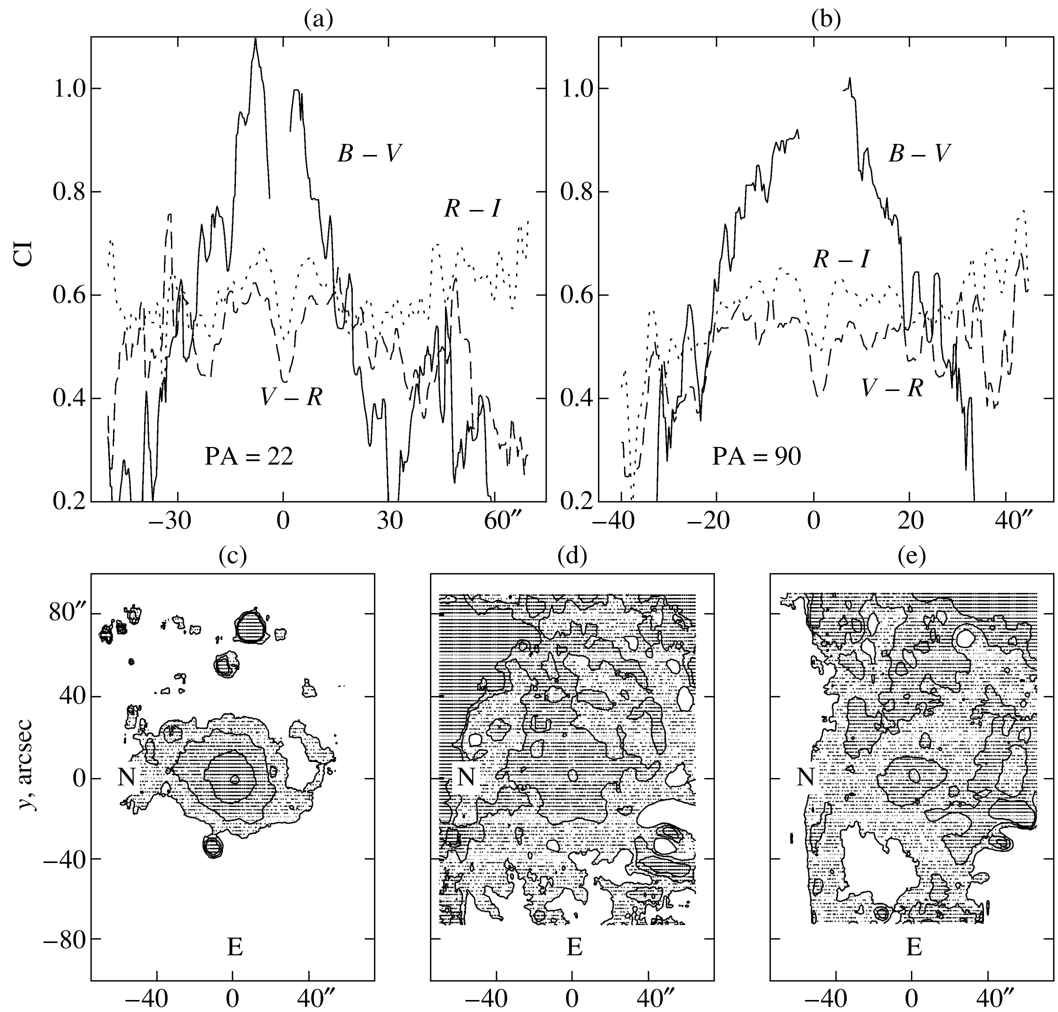

Fig. 5. The $B-V$ (solid line), $V-R$ (short-dashed line), and $R-I$ (dotted line) color indices (a) along the major axis of the galaxy and (b) along the major axis of the bar, together with maps of the (c) $B-V$, (d) $V-R$, and (e) $R-I$ color indices. Contours of equal color indices of 0.4, 0.6, and 0.8 (c); 0.3, 0.5, and 0.7 (d); and 0.4, 0.6, and 0.8 (e) are indicated; the dark intervals correspond to larger color indices.

The star-formation rate (SFR) in NGC 3184 is fairly high: SFR $= 1.4 \pm 0.1 M_\odot$/year according to IR observations and $0.5 \pm 0.05 M_\odot$/year according to Hα observations [11, 18]. The star-formation efficiency (SFE) in the galaxy is SFE $= (5.6 \pm 0.2) \times 10^{-10}$ year^{-1} from IR observations and SFE $= (1.4 \pm 0.1) \times 10^{-10}$ year^{-1} from Hα observations [11, 18].

3.4. Sites of Star Formation in the Galaxy

We have identified 13 modest star-like and diffuse blue formations in the outer regions of the disk and in the spiral arms of NGC 3184. Their position in the $(B-V)_0^i-(V-R)_0^i$ and $(B-V)_0^i-(V-I)_0^i$ two-color diagrams is shown in Figs. 6b, 6d. The columns of Table 3 present the derived parameters for these objects: (2) their coordinates relative to the galactic center in arcseconds, (3)–(5) $(B-V)_0^i$, $(V-R)_0^i$, and $(V-I)_0^i$ color indices, (6) Hα luminosity $10^3 L_\odot$, (7) the diameter of the region in parsecs, and (8) their age in units of 10^6 yrs. When deriving the color indices of the regions, we determined their brightnesses in each filter by subtracting the background radiation of the surrounding disk from the radiation coming from the region of the site of star formation. The ages of the star-forming regions were estimated from their positions in the two-color diagrams, using evolutionary tracks for aging stellar systems with $Z = Z_\odot$ obtained with the PEGASE2 code [2].

The average size of the star-forming regions in NGC 3184 is 120–170 pc. Some star-forming regions in the galaxy display complex hierarchical structures: two to three brighter regions with diameters of 120–180 pc are visible within regions

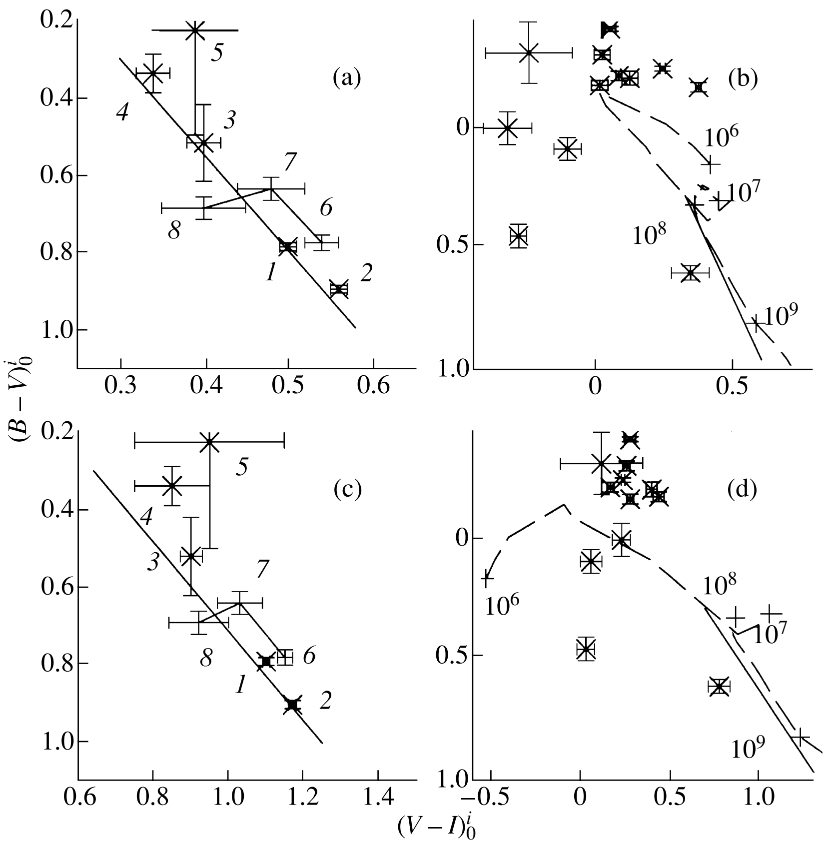

Fig. 6. (a, b) $(B-V)_0^i-(V-R)_0^i$ and (c, d) $(B-V)_0^i-(V-I)_0^i$ two-color diagrams for (a, c) some regions of NGC 3184 and (b, d) sites of star formation in the galaxy. The straight solid lines represent the normal color sequences (NCS) for galaxies, according to [25]. The broken solid lines in the left graphs indicate variations of the color indices along the major axis of the bar. The dashed curves in the right graphs are evolutionary tracks for a stellar system without star formation and with $Z = 0.02$ (the age in years is indicated). The errors are indicated. The shift due to selective dust absorption is parallel to the NCS. The numbers denoting different regions of NGC 3184 are explained in the text.

230 ± 60 pc in size; this is true, for example, of star-forming regions 8 and 10 (see Table 3). The sizes of most sites of star formation in NGC 3184 are typical of stellar associations; the sizes of two regions (3, 5) indicate that they are stellar aggregates (according to the hierarchical star-formation scale of Efremov [27]).

In the $(B-V)_0^i-(V-R)_0^i$ and $(B-V)_0^i-(V-I)_0^i$ two-color diagrams, a substantial fraction of the star-forming regions are located along the evolutionary track of a young stellar system with an age of about $(3–7) \times 10^6$ yrs. Some clusters are located appreciably above this track (Figs. 6b, 6d). This may indicate a significant contribution from non-stellar radiation associated with these star-forming regions, such as radiation by hot gas. Clusters 5 and 13 in the diagrams are situated to the left of the evolutionary track, possibly due the fact that we have not taken dust into account in these regions. The luminosity of most of the objects is $L(\mathrm{H}\alpha) = (1–4) \times 10^4 L_\odot$.

Region 3 is the bright star-like object that is connected to the central regions of the galaxy by a bridge (see Section 3.1). Judging from its photometric parameters and intense Hα radiation (Table 3), this object is a stellar aggregate with a diameter of 260 pc. The position of region 3 in the two-color diagrams indicates that it may be a young object with very strong selective absorption, ($E(B-V) = 1.5^m$). This is also supported by the fact that the infrared color indices of the region obtained from JHK photometry from the 2MASS survey are $J-H = 0.33^m \pm 0.10^m$ and $H-K = 0.07^m \pm 0.10^m$, which corresponds to an age of $(6.8 \pm 1.3) \times 10^6$ yrs.

Object 8 (probably the youngest of those studied) is distinguished by its very intense Hα luminosity, $1.68 \times 10^5 L_\odot$ (46% of the core luminosity of NGC 3184).

We have not been able to determine the age of region 2 with confidence, due to the absence of data on selective absorption in this region. In the absence of appreciable absorption, the age of the stellar population of this region is $(6.5–30) \times 10^8$ yrs (depending on the chemical composition). It is possible that we

Table 3. Parameters of sites of star formation in the galaxy

No.	Coordinates, arcsec	$(B-V)_0^i$	$(V-R)_0^i$	$(V-I)_0^i$	$L(H\alpha)$, $10^3 L_\odot$	d, pc	t, 10^6 yrs
1	59.6N, 4.9E	−0.31	−0.27	0.07	17	80	4.8 ± 1.0
2	70/2N, 43.7E	0.63	0.32	0.72	16	155	7.5–3000
3	10.5N, 31.2E	1.26	0.12	0.32	41	260	6.8 ± 1.3?
4	37.2S, 18.9E	0.01	−0.35	0.18	9	140	5.5 ± 0.3
5	50.7S, 1.9E	0.10	−0.13	0.01	27	235	5.0 ± 1.0
6	58.4S, 35.5W	−0.30	0.00	0.21	11	120	4.8 ± 1.0
7	55.1S, 53.8W	−0.17	−0.01	0.39	14	120	5.3 ± 1.4
8	27/6S, 67.7W	−0.24	0.22	0.19	168	170	4.3 ± 1.3
9	14.1S, 78.4W	−0.20	0.10	0.35	29	120	4.8 ± 1.5
10	1/3N, 56.0W	−0.21	0.06	0.12	25	140	4.7 ± 1.0
11	7.9N, 78.4W	−0.16	0.35	0.23	32	160	5.0 ± 2.1
12	25.5N, 64.1W	−0.41	0.03	0.23	14	120	4.8 ± 1.1
13	49/3N, 17.5W	0.47	−0.31	−0.02	11	140	<5

are dealing here with a moderately old stellar cluster or a dwarf galaxy.

Larsen [17] studied 13 other young stellar clusters in NGC 3184 in the U, B, V, and I bands. We derived the ages of these objects from his $U-B$, $B-V$, and $V-I$ color indices using model evolutionary tracks calculated with the PEGASE2 code [26]. Table 4 presents the resulting ages. For at least ten of the objects studied by Larsen [17], the ages are similar to those of the sites of star formation considered here.

As was already noted in Section 1, about 100 HII regions are known in NGC 3184. Here, we were not able to use the spectrophotometric observations of HII regions from [13–14], since those regions are situated near the periphery of the galaxy and lie outside the field of view of our CCD camera. However, there are also many HII regions in the inner region of the galaxy (Fig. 2d). Their sizes are $2''$–$8''$ (80–310 pc), which correspond to stellar associations and aggregates (according to the classification of Efremov [27]). It is possible that the galaxy contains HII regions smaller than $2''$, but we cannot test this due to the insufficient quality of our Hα images. Several groups of close HII regions are seen, which form chains and rings. The characteristic scale for these formations is $12''$–$20''$ (480–800 pc), which corresponds to the sizes of stellar complexes [27], and is also the characteristic width of the spiral arms of NGC 3184 (Fig. 2d).

4. DISCUSSION

On the whole, NGC 3184 is a typical late-type galaxy with ongoing star formation in the disk and possibly in the core. The star formation in the galaxy is of a quiescent (non-burst) type. An appreciable fraction of young stars are located in compact star-forming regions. At least three spatial star-formation scales can be recognized in NGC 3184: (1) chains and rings with characteristic sizes 500–800 pc, (2) diffuse and star-like regions with diameters of 200–300 pc, and (3) star-like regions with diameters of 80–200 pc. These results are consistent with the hierarchical scale of star-formation suggested by

Table 4. Ages of young stellar clusters in NGC 3184

No.	Name (from [17])	t, 10^6 yrs
1	n3184–105	6.6 ± 0.4
2	353	6.3 ± 0.9
3	383	6.8 ± 0.3
4	475	6.3 ± 1.0?
5	568	5.9 ± 0.4
6	788	7.4 ± 0.2
7	870	7.3 ± 0.9
8	878	250 ± 60
9	909	6.8 ± 0.9
10	1053	6.5 ± 0.5
11	1070	5.9 ± 0.4
12	1137	8.2 ± 0.8
13	1316	6.2 ± 0.2

Efremov [27] (complexes—aggregates—associations); however, no distinct boundary between stellar aggregates and associations can be seen in NGC 3184. Both star-like aggregates and aggregates containing several stellar associations are seen in the galaxy; both types of aggregates display the same color indices.

The ages of the young star-forming regions in the galaxy are $(4–7) \times 10^6$ yrs, possibly due to a selection effect, if this is the age at which clusters of a given equal mass display the maximum B luminosity.

Spectrophotometric observations are needed to clarify the nature of the bright star-like object located in the eastern part of the galaxy. Our data do not provide an unambiguous answer to the question of whether the object is a field star or belongs to NGC 3184. The origin of the bridge toward the object also remains unclear. Clarification of these issues requires analyses of the kinematics of the galaxy, and, most of all, mapping of the velocity field of NGC 3184. Thus, in spite of the large volume of data already available for NGC 3184, supplementary studies are needed.

5. CONCLUSIONS

(1) The disk brightness of NGC 3184 decreases exponentially with a characteristic scale of $51.7'' \pm 4.5''$ (2.02 ± 0.17 kpc); the brightness of the bulge decreases according to a de Vaucouleurs law with effective radius $23.2'' \pm 3.7''$ (0.91 ± 0.14 kpc).

(2) The galaxy displays active, though quiescent (non-burst), star formation, i.e., star formation occuring at a constant rate. The only region where star formation is not currently observed is the bulge.

(3) Three scales of star-formation can be distinguished: complexes (characteristic size 500–800 pc), aggregates (200–300 pc), and associations (80–200 pc). The ages of the brightest star-formation regions in the galaxy are $(4–7) \times 10^6$ yrs.

ACKNOWLEDGMENTS

The authors are grateful to A.V. Zasov (Sternberg Astronomical Institute) for useful discussions and comments, and to D.V. Bizyaev (Sternberg Astronomical Institute) for the preliminary reduction of the observations. This work was partially supported by the Russian Foundation for Basic Research, project nos. 98-02-17102, 01-02-16800, and 01-02-17597. This study was based partially on data from the Isaac Newton Group Archive (Cambridge).

REFERENCES

1. G. de Vaucouleurs, A. de Vaucouleurs, H. G. Corwin, *et al.*, *Third Reference Catalogue of Bright Galaxies* (Springer-Verlag, New York, 1991).
2. R. W. Pogge, Astrophys. J., Suppl. Ser. **71**, 433 (1989).
3. S. van den Bergh, Astron. J. **110**, 613 (1995).
4. W. E. Baggett, S. M. Baggett, and K. S. J. Anderson, Astron. J. **116**, 1626 (1998).
5. P. J. Grosbol, Astron. Astrophys., Suppl. Ser. **60**, 261 (1985).
6. D. M. Elmegreen and B. G. Elmegreen, Astrophys. J. **314**, 3 (1987).
7. P. Martin and J.-R. Roy, Astrophys. J. **424**, 599 (1994).
8. P. Martin, Astron. J. **109**, 2428 (1995).
9. D. M. Elmegreen, B. G. Elmegreen, F. R. Chromey, *et al.*, Astron. J. **111**, 1880 (1996).
10. D. M. Elmegreen, B. G. Elmegreen, F. R. Chromey, *et al.*, Astron. J. **111**, 2233 (1996).
11. L. Martinet and D. Friedli, Astron. Astrophys. **323**, 363 (1997).
12. P. W. Hodge, Astron. J. **87**, 1341 (1982).
13. M. L. McCall, P. M. Rybski, and G. A. Shields, Astrophys. J., Suppl. Ser. **57**, 1 (1985).
14. D. Zaritsky, R. C. Kennicutt, Jr., and J. Huchra, Astrophys. J. **420**, 87 (1994).
15. L. van Zee, J. J. Salzer, M. P. Haynes, *et al.*, Astron. J. **116**, 2805 (1998).
16. S. S. Larsen and T. Richtler, Astron. Astrophys. **345**, 59 (1999).
17. S. S. Larsen, Astron. Astrophys., Suppl. Ser. **139**, 393 (1999).
18. J. S. Young, L. Allen, J. D. P. Kenny, *et al.*, Astron. J. **112**, 1903 (1996).
19. W. Cui, W. T. Sanders, D. McCammon, *et al.*, Astrophys. J. **468**, 102 (1996).
20. R. Barbon, E. Cappellaro, and M. Turatto, Astron. Astrophys., Suppl. Ser. **81**, 421 (1989).
21. D. W. E. Green, IAU Circ. **7334**, 1 (1999).
22. I. I. Zin'kovskiĭ, S. S. Kaĭsin, A. I. Kopylov, *et al.*, *Technical Report of Special Astronomical Observatory, Russian Academy of Sciences,* 1994, No. 231.
23. S. R. Majewski, R. G. Kron, D. C. Koo, and M. A. Bershady, Publ. Astron. Soc. Pac. **106**, 1258 (1994).
24. P. Prugniel and P. Heraudeau, Astron. Astrophys., Suppl. Ser. **128**, 299 (1998).
25. R. Buta and K. L. Williams, Astron. J. **109**, 543 (1995).
26. M. Fioc and B. Rocca-Volmerange, Astron. Astrophys. (in press) (2001).
27. Yu. N. Efremov, *Sites of Star Formation in Galaxies* [in Russian] (Nauka, Moscow, 1989).

Translated by K. Maslennikov